

Multi-response Optimization of PMEDM on Inconel 718 Using Hybrid T-GRA, TOPSIS, and ANN Model

Jana Sai Ram

Department of Mechanical Engineering
B. S. Abdur Rahman Crescent Institute of
Science and Technology
Chennai
India

Jeavudeen Shiek

Department of Mechanical Engineering
B. S. Abdur Rahman Crescent Institute of
Science and Technology
Chennai
India

Shaul Hameed Syed

Department of Mechanical Engineering
B. S. Abdur Rahman Crescent Institute of
Science and Technology
Chennai
India

Inconel 718 is one of the Nickel-based superalloys considered one of the most difficult-to-machine materials owing to its property to retain hardness at higher temperatures. This study examined the performance of Eductor-based PMEDM machining on Inconel 718. Taguchi L9 OA has been used with current, Pulse-OFF time & Pulse-ON time as process parameters with a delivery side pressure of 6 bar for the Alumina mixed dielectric. Material removal rate (MRR), Tool wear rate (TWR), & surface roughness (SR) have been taken as output responses. The results have been investigated by MADM techniques, namely Taguchi-based Grey Relational Analysis (T-GRA) & TOPSIS analysis. Furthermore, the ranks obtained from T-GRA & TOPSIS have been validated by developing a single-layered ANN model. Ranks predicted by the ANN model are the same for T-GRA and TOPSIS and the R-values are 0.924 & 0.871, respectively. ANOVA has also been used to analyze parameter effects on output responses.

Keywords: Multi-attribute Decision Making, T-GRA, TOPSIS, ANN, PMEDM, MRR, TWR, SR.

1. INTRODUCTION

Electrical discharge Machine (EDM) is widely used to accurately imprint the intricate shapes of the tools that will be machined into the workpiece. When components need to be manufactured with finer tolerances, the EDM is established as a precision machining method. In EDM the material is removed by melting and vaporisation of the work material in the machining area. This results in heat production between the gaps. A significant amount of heat is released between the gaps with an approximate temperature of 8000–12,000°C by the conversion of thermal energy into sparking energy [1].

In traditional machining, the relative motion between the cutting tool and the work piece results in friction and considerable tool wear. This hinders the machinability in traditional machining due to the mechanical characteristics of the work material. In EDM, there is no direct contact between the tool and the work piece [2], but the materials should be electrically conductive whereas in the conventional machining some constraints are built-in such as vibration, residual stresses which are eliminated [3]. This prompts tool makers to prefer EDM to machine complicated patterns and profiles on dies & moulds with greater dimensional accuracy [4]. Moreover, EDM is preferred to unconventional methods because it is independent of the relative hardness between the tool and the workpiece. In EDM, the material is removed by a spark erosion mechanism, which removes the workpiece in the respective shape of the tool [5].

Srinivasan et al. [6] discussed the dependent parameters like current, pulse on time, pulse off time, dielectric pressure, and gap voltage that play a prime role in deciding the output responses like MRR, TWR, & Ra. Sen and Mondal [7] conducted experiments using various tools like copper, brass, and graphite with mild steel IS2062 as the workpiece, where it was observed that out of these parameters like peak current, spark voltage, dielectric flushing, & pulse on time the peak current played a significant effect on removal rate, tool wear rate, and surface finish.

In powder-mixed EDM (PMEDM), the dielectric is combined with powder additives in the form of fine particles, and the resulting combination is then admitted into the spark gap between the tool and the work piece, which has been observed to improve the process' machinability [8]. With different concentrations of Alu-minum powder mixed with drinking water, Gugulothu et al., [9] conducted experiments based on L₂₇ OA with Inconel 718 and noticed that MRR was maximum with 6gm/l of powder concentration. Jeavudeen et al., [10] conducted Taguchi L₁₈ experiments with Alumina, Silica, and Copper and found that Eductor based EDM was efficient in mixing powders uniformly in dielectric. Jafrey Daniel et al. investigated the composite material, and the test was designed using L₂₇ Orthogonal Array with 4 input parameters such as pulse on time, pulse of time, wire feed, and wire tension. As a result, it was observed that MRR and SR were found to be appreciated outcomes using the MCDM technique [11].

Inconel is difficult to machine due to its high toughness, hardness, work hardening rate, and poor thermal properties [12]. A. Singh et al., [13] used Technique for Order of Preference by Similarity to Ideal

Received: July 2023, Accepted: September 2023

Correspondence to: Dr. S. Jeavudeen, Department of
Mechanical Engineering, B. S. Abdur Rahman Crescent
Institute of Science and Technology, Chennai, India.

E-mail: shiek.zia@gmail.com

doi: 10.5937/fme2304564R

Solution (TOPSIS) with five types of weight criterion, viz., mean weight, standard deviation, entropy, analytic hierarchy process (AHP), and Fuzzy on Inconel 718 as work material and Tungsten as tool electrode. In their study, the uncertainty in the decision making was explored by fuzzy weighing approach. According to payal et al., [14] experiments were conducted on Inconel 625 super alloy, with copper-tungsten electrodes yielding the best results for MRR & TWR in EDM. Bharti et al., [15] discovered that the discharge current had the greatest effect on all performance indicators. It was found that MRR, Ra, and EWR might all be affected by changing the discharge current and the pulse-on time. The experimental results from EDM on Inconel 718 demonstrated that increasing the pulse length to 750 μ s enhanced MRR. Hussain et al., [16] used Inconel 625 as the workpiece to optimize process parameters such as Ton, Ip, and Toff to maximize MRR. Analysing the machinability of EDM involves multiple input parameters and output responses. This necessitates using the various optimization techniques & statistical tools for better understanding of the results. The design of experiment (DOE) was developed by R.A. Fisher as a statistical tool for studying the simultaneous effects of multiple variables and conducted the first experiment to determine how much sunlight, fertiliser, water, etc. were needed to grow a productive crop. Taguchi's technique and Full Factorial Design (FFD) are the two basic DOE strategies [17].

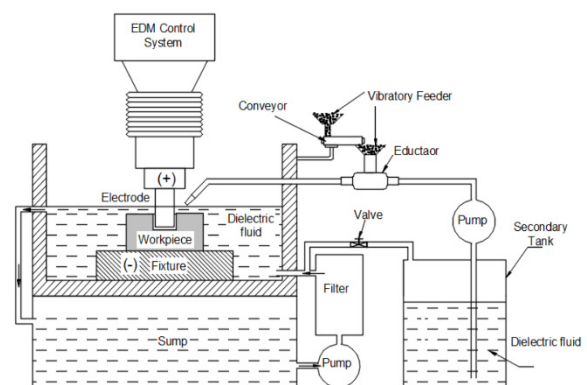
Balakrishnan Deepanraj et al., [18] conducted experiments on selected process parameters like cutting speed, feed rate, depth of cut to get the surface roughness as an output by using Taguchi L9 OA design on AISI 4340 steel as a workpiece. Therefore, it was observed that the most contribution factor to get surface roughness was feed rate 70.50% and followed by depth of cut (18.54%) and cutting speed (9.15%). Srinivasan et al. [19] conducted experiments with three machining parameters, namely current, pulse on time, and spark gap voltage, to get the output responses like MRR and EWR using the Taguchi method and found that current was the most influential factor to increase the MRR and decrease the TWR. Singh et al., [20] conducted experiments with high strength low alloy (HSLA) steel used as a workpiece in EDM and investigated the

impacts of process variables on the tool wear rate (TWR). Taguchi method was employed for designing the experiments to study the impact of Current, Pulse off time, and pulse on time. According to their findings, current (82.75%) was the factor that affected tool life the most.

According to Ramamurthy et al. [21], the 3 different types of wire-electrodes, namely brass wire, zinc-coated wire, and diffused coated brass wire, were used to conduct the experiments on Ti-6Al-4V alloy (workpiece) based on Taguchi L₉ orthogonal array in WEDM. It was observed that the pulse of time influenced more in diffused brass wire, which produced the lower SR with minimum kerf width. Based on Hadi et al. [22], it was reported that experiments were conducted with 3 different tools, namely copper, graphite, and copper-graphite, on MONEL 400, and it was found that the copper-graphite tool gave optimal results in terms of MRR and Ra. Jeavudeen et al. [23] investigated the effect of three process parameters (gap duty, duty cycle, and flow rate of PM) with aluminum and mild steel (workpiece) by using copper (12 mm dia) as an electrode. They observed that the parameters increase showed the MRR rise (17.52%) in Aluminum and TWI low (4.08%) in mild steel using L9 OA design. In the multi-objective optimization using L9 orthogonal of WEDM, current was the most influential factor, with 78.42%, followed by voltage [24]. Deangan et al. [25] used copper wire of 0.25 mm diameter with distilled water as dielectric and observed higher MRR by altering the input parameters combination such as pulse on time, Wire feed, and Pulse off Time. Mandal et al. [26] conducted experiments on the EDM with the copper electrode, uncoated aluminum, and copper-coated electrode and reported that copper performed better in machining output than uncoated copper. MRR increased by 24%, EWR decreased by 23% with the copper electrode, whereas the SR was better with the coated copper electrode. Mukherjee et al. [27] experimented with the two forms of tools with current, discharge time, and discharge voltage as processing inputs. They found that the current was the most influential factor in the effect of the wear rate at the inner edge of the hollow tool and front wear for the chamfer tool.



(a) Experimental setup



(b) Schematic diagram

Figure 1. Experimental set-up (a) and Schematic representation of EDM (b)

Balasubramanian et al. [28] conducted experiments on two different workpiece materials, namely EN8 and D3 steel, with two different tool forms and detected that both the work materials experienced higher MRR and lower TWR. Yuangang et al. [29] investigated micro-feature tools and compared them with the block's drilled chambers. The current, pulse width, and pulse interval effects on response variables (tool bottom side length, tool length, material removal rate, surface roughness, and side length deviation rate) were discussed.

Rajneesh Kumar Singh et al. [30] explained the process parameters like working gap, abrasive weight, voltage, and rotational speed effects on improving the surface quality of aluminum 6060 using Taguchi-based hybrid meta-heuristic SA-GRA design. Based on GRA results, the contribution effect was obtained on voltage (59.75%) followed by abrasive weight (22.73%), working gap (5.07%), and rotational speed (0.06%).

Kumar and Mondal [31] utilized optimization techniques like TOPSIS and GRA and reported that improvements were found in each output response (MRR, SR, TWR) with these MCDM techniques. In the study of tungsten-copper tools and Si3N4-TiN as workpiece, to examine responsive characteristics like MRR, TWR, SR and geometrical tolerances, MCDM methods like GRA and TOPSIS were used to maximise response efficiency [32]. Using a brass tube tool, Rajmanickam et al., [33] investigated on EDM of Ti-6Al-4V workpiece with RSM- CCD method and TOPSIS as multi objective optimization technique. Bhaumika et al., [34] employed RSM with TOPSIS and $MRR = \frac{Wb - Wa}{t}$

GRA as MCDM technique to determine the optimal parameter setting for the EDM of titanium grade 6 alloy.

Some researchers have attempted to construct a model using various complex processing techniques in order to predict the machining process [35]. The artificial neural network (ANN) has been considered to be one of the modeling tools utilized to forecast desired performance in EDM [36]. Tsai and wang [37] created neural network models for EDM process parameter prediction and achieved compatible results. By combining the work with an AI tool, artificial neural networks can shed fresh light on the investigation of several fundamental fields. Due to the relative novelty of this area of study, there is a very limited amount of literature available to guide the development of effective manufacturing responses. Somchai Kongnoo et al. conducted research on the springback angle of ASTM A-210 Gr during bending and compared the results with those obtained by an artificial neural network (ANN) with a Sigmoid (R- 99.42%), ReLU (R- 98.99%), TanH (R- 99.53%), Identity function (R- 79.53%). Results were compared by taking the neural network architecture as 4 neurons in the input layer, 98 in the hidden layer, and 1 in the output layer, and the calculated error was 0.001892 [38]. According to the findings, a multilayer preceptor neural network model with three hidden layers reasonably forecasted the SR under a variety of machining conditions.

Though the researchers have experimented with the machining of Inconel alloy with PMEDM, the present

work emphasizes the use of ANN for predicting Ranks rather than MADM algorithms. The use of the Eductor-based PMEDM method is one of the techniques to have a thorough and uniform mixing of Alumina powders in the dielectric at the time of machining. Besides, the Eductor can be a replacement for the one-step method (viz., stirring mechanism) and two-step method (viz., stirring and surfactant) for dispersing in dielectric & stabilizing the powders in dielectric. Optimization has been carried out by comparing multi-attribute decision-making methods (MADM), namely Taguchi-based Grey Relational Analysis (T-GRA), and the technique for Order of Preference by Similarity to Ideal Solution (TOPSIS) with the ANN method.

2. EXPERIMENTAL WORK

In the present work, Inconel alloy (60 x 60 x 10 mm) has been used as the workpiece with a circular copper tool diameter of 10mm as the tool electrode. Since the Eductor-based PMEDM set-up could mix any powder regardless of its type and particle size, the EDM machine (Electronica Make, India) is customized to perform these experiments. Figure. 1(a) [10] depicts the experimental set-up, and a schematic portrayal is shown in Figure. 1(b). As seen in Table 1, the operational conditions of the machining are specified in the tabular form. Three machining parameters, viz., peak Current, Pulse on Time, and Pulse off time, have been chosen as variables, while other variables are held constant. Utilizing an electronic balance (Metler, India), the weight loss method has been used to calculate the material removal rates for the tool and the workpiece. To calculate the MRR and TWR, the following expressions (1) & (2) have been used:

$$MRR = \frac{Wb - Wa}{t} \quad (\text{gm/min}) \quad (1)$$

$$TWR = \frac{Eb - Ea}{t} \quad (\text{gm/min}) \quad (2)$$

where,

W_b is Weight of the workpiece before machining.

W_a is weight of the workpiece after machining.

t is Machining time.

E_b is weight of the tool before machining.

E_a is weight of the tool after machining.

Table 1. Experimental condition for the machining operation

S.No	Machining Parameter	Description	Unit
1	Dielectric medium	Alumina mixed dielectric	-
2	Polarity	Positive	-
3	Tool material	Copper	-
4	Forms of Tool	Round	-
5	Machining time	10	mins
6	Current	25,30,35	A
7	P on time	3,6,9	μ Sec
8	P off time	20,25,30	μ Sec
9	Delivery Pressure at the Eductor	6	bar

The experiment's design was based on a 3-factor and 3-level Taguchi L₉OAs in Table. 2. The observations are given in Table 3. The workpiece's surface after the experimental trials is shown in Figure 2.

Table2. Machine control settings

S.No	Parameter	Level 1	Level 2	Level 3
1	Current (amps)	25	30	35
2	P off time (μ Sec)	20	25	30
3	P on time (μ Sec)	3	6	9

Table3. Experimental observations

Run	Current	T _{OFF}	T _{ON}	MRR (gm/min)	TWR (gm/min)	SR (μm)
1	25	20	3	1.10	0.06	6.44
2	25	25	6	0.45	0.12	10.82
3	25	30	9	1.18	0.08	9.37
4	30	20	6	1.89	0.27	7.19
5	30	25	9	1.55	0.27	9.50
6	30	30	3	0.61	0.09	8.77
7	35	20	9	2.53	0.30	7.07
8	35	25	3	0.38	0.07	8.76
9	35	30	6	0.73	0.05	11.84



Figure 2. Machined surfaces of the workpiece

2.1 Optimization Techniques

Since MRR, TWR, and SR are three output responses, the application of MADM concepts has been employed in solving decision-making based on many criteria. All types of enterprises can effectively manage their project risk by utilizing these approaches to make decisions involving multiple attributes or responses. The primary components of a MADM problem are the criteria and the options.

Various alternatives have been evaluated against predetermined standards to provide a comparison of alternatives. As the importance might fluctuate greatly from one decision-maker to another, weighing diverse variables will help the findings even more. Because of this, some criteria' importance may vary from one person's perspective to another. Therefore, from the perspective of various decision-makers, there may be a variable amount of priority for certain criteria [39]. In this research, to get the optimal solution for the given multi-attribute, namely MRR, TWR, and SR, Taguchi-based GRA (T-GRA) and TOPSIS methods have been used, and they are discussed below:

2.2 ANN

Artificial Neural Network (ANN) is a significant model which employs learning of linear and non-linear problems in many engineering domains. Many factors, including ANN architecture and ANN training parameters, must be considered to create inferences and a robust ANN. The key design choices have a role to play in the performance of ANN in getting the desirable output [40]. ANNs are made up of several interconnected processors working in parallel where experimental data involves modifying system workloads and abilities to minimise the difference between the actual and the predicted outputs [41]. In this research, MATLAB has been used to create ANN models for the given experimental data. This helps in developing statistical techniques in getting desirable requirements in EDM machining.

2.3 Grey Relational Analysis Method

Deng developed grey relationship analysis and it works with a certain idea of information to get the optimal solution in the case of multiple responses [42]. In GRA, experimental data are first normalised, and the original sequence is changed to a compatibility sequence. The expressions (3) and (4) are used to normalize the initial sequence for 'the higher, the better' and 'the smaller, the better' characteristics. Table.4 shows the grey-scale normalised data for MRR, TWR, and SR.

$$X^*i(k) = \frac{Y_i(k) - \min y_i(k)}{\max y_i(k) - \min y_i(k)} \quad (\text{larger-the-better}) \quad (3)$$

$$X^*i(k) = \frac{\max y_i(k) - Y_i(k)}{\max y_i(k) - \min y_i(k)} \quad (\text{larger-the-better}) \quad (4)$$

where,

Min $y_i(k)$ = smallest $y_i(k)$ value.

Max $y_i(k)$ = largest value of the $y_i(k)$.

$X^*i(k)$ = normalization compatibility sequence.

Table4 Grey Normalized values of MRR, TWR, and SR

S.No.	Experimental Values			Normalized Values		
	MRR	TWR	SR	MRR	TWR	SR
1	1.1	0.06	6.44	0.335	0.040	1.000
2	0.45	0.12	10.82	0.033	0.280	0.190
3	1.18	0.08	9.37	0.372	0.120	0.458
4	1.89	0.27	7.19	0.702	0.880	0.861
5	1.55	0.27	9.50	0.544	0.880	0.433
6	0.61	0.09	8.77	0.107	0.160	0.569
7	2.53	0.3	7.07	1.000	1.000	0.883
8	0.38	0.07	8.76	0.000	0.080	0.570
9	0.73	0.05	11.84	0.163	0.000	0.000

The link between the ideal and the actual normalized data is calculated using the Grey Relational Coefficient (GRC). The formula for calculating the grey relational coefficient is $\xi_i(k)$ and is shown in (5):

$$\xi_i(k) = \frac{\Delta_{\min} + \mu\Delta_{\max}}{\Delta_{0i}(k) + \mu\Delta_{\max}} \quad (5)$$

where,
 $\xi_i(k)$ = Grey relational coefficient,
 μ = identification coefficient ($0 \leq \mu \leq 1$), and its value is taken as 0.33.
 Δ_{\min} = smallest value of the $\Delta_{0i}(k)$ and
 Δ_{\max} = largest value of the $\Delta_{0i}(k)$
 Deviation Sequence can be calculated as shown in (6).

$$Hi = \frac{S^-}{S^+ + S^-} \quad i = 1, 2, 3, \dots, m \quad (6)$$

where,
 $\Delta_{0i}(k)$ = deviation sequence,
 $X^*_o(k)$ = Deviation among $X^*_o(k)$ and $X^*_i(k)$, ($X^*_o(k)$ is taken as 1)

For each output response, the grey relational coefficient (GRC) was determined using (5), and the GRG was then estimated as given in (7). The GRC, GRG, and rank were obtained by grey relational analysis, shown in Table 5.

The formula of the grey relational coefficient, which is used to calculate the grey relational grade, is shown in (7):

$$\gamma_i = \frac{1}{n} \sum_{K=1}^n \xi_i(k) \quad (7)$$

where,
 n = number of process responses,
 γ_i = Grey relational grade
 $\xi_i(k)$ = Grey relational coefficient.
 After obtaining the rank, the average GRG is given in Table 5.

Table5. GRC, GRG, and Rank

S.No	Grey Relational Coefficient			GRG	Rank
	MRR	TWR	SR		
1	0.332	0.256	1.000	0.529	3
2	0.254	0.314	0.290	0.286	8
3	0.345	0.273	0.379	0.332	5
4	0.526	0.733	0.704	0.654	2
5	0.420	0.733	0.368	0.507	4
6	0.270	0.282	0.433	0.328	6
7	1.000	1.000	0.737	0.912	1
8	0.248	0.264	0.434	0.315	7
9	0.283	0.248	0.248	0.260	9

2.4 Grey-based ANN design

Significant developments have occurred across the field of engineering due to the widespread adoption of AI tools in recent years to achieve higher quality and improve production. In an effort to construct a model from the experimental data, several researchers have employed various statistical methods [43]. One such is ANN, which can be trained to overcome the constraints of traditional methods towards resolving issues.

In this work, MATLAB, which has been used to construct a precise neural network model, is shown in Figure 3. The developed model includes one input layer with three neurons, namely MRR, TWR, and SR. The network's topology can be written as [3, HL1,1], where HL1 represents the 10 hidden-layer nodes. The network topology has been arranged in [3,10,1], and all the weights have been initially assigned randomly via the MATLAB input function. The T-GRA & TOPSIS data

is considered as training data to the ANN model ReLu activation function. Arranging each 3 input neurons to the 10 nodes of the hidden layer will result in output by the summation of the weights and bias. By continuously adding 10 neurons to the hidden layer, the network has been able to reach the final output of [3, 10, 1].

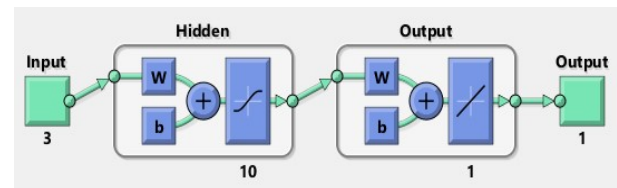


Figure 3. Network Scheme used in ANN.

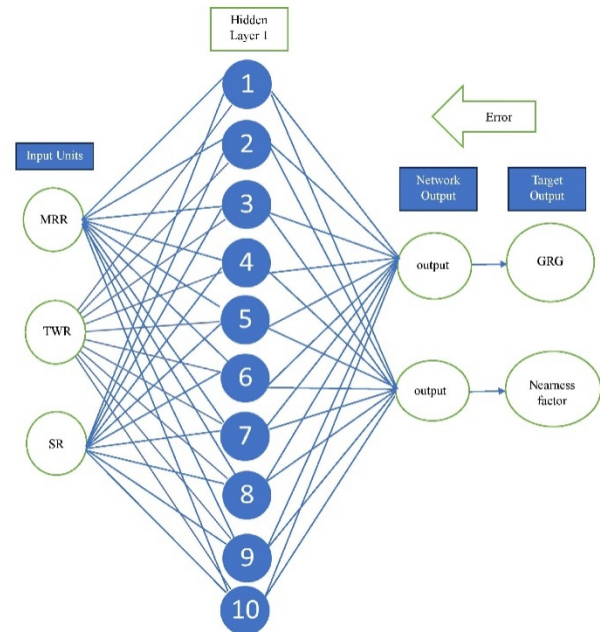


Figure 4. Feed Forward Back Propagation network structure

Table6. Actual and ANN Predicted GRG

S.No	GRG Actual	One Layer	
		GRG-ANN predicted	Error
1	0.529	0.2988	0.23034190
2	0.286	0.2223	0.06373587
3	0.332	0.3319	0.00000001
4	0.654	0.6544	0.00000002
5	0.507	0.5071	0.00000002
6	0.328	0.3427	0.01431782
7	0.912	0.7856	0.12691475
8	0.315	0.3155	0.00000000
9	0.260	0.2597	0.00000007

Table 7. Mean of the grey relational grade overall (GRG)

S.No	Level	Current	T _{on} time	T _{off} time
1	1	0.3823	0.6983	0.3907
2	2	0.4963	0.3693	0.4000
3	3	0.4957	0.3067	0.5837
4	Delta	0.1140	0.3917	0.1930
5	Rank	3	1	2

This process is repeated until it yields a minimum error. The network structure used for the ANN is shown in Figure 4. Using ANN, the actual GRG is validated

with ANN outputs, and the same is shown in Table 6. Table 7 shows the overall mean grade of GRG is found to be higher at “pulse on time” when compared to “Current” and “Pulse off time”.

2.5 TOPSIS

TOPSIS is one of the MADM methods to obtain the optimal results for the multi-attribute systems. Bhuyan et al. explain that the TOPSIS yields a solution that is both closest to the ideally best result and farthest from the hypothetically worst result. The objective is to identify a solution using the nearness factor between the feasible and the ideal solutions [44]. The TOPSIS approach involves the following steps:

The first stage in this process is to create a decision matrix (D) as given in (8) with m rows and n columns.

$$D = \begin{bmatrix} Q_{11} & Q_{12} & Q_{13} & \dots & \dots & Q_{1n} \\ Q_{21} & Q_{22} & Q_{23} & \dots & \dots & Q_{2n} \\ Q_{31} & Q_{32} & Q_{33} & \dots & \dots & Q_{3n} \\ \vdots & \vdots & \vdots & \ddots & \ddots & \vdots \\ \vdots & \vdots & \vdots & \ddots & \ddots & \vdots \\ Q_{m1} & Q_{m2} & Q_{m3} & \dots & \dots & Q_{mn} \end{bmatrix} \quad (8)$$

where,

m = No. of experiments,

n = output response of every experiment.

In the second stage, the normalized matrix (E_{ij}) is determined using the relation shown in (9)

$$E_{ij} = \frac{Q_{ij}}{\sqrt{\sum_{i=1}^m Q_{ij}^2}} \quad (9)$$

where,

Q_{ij} = Input of decision matrix (for $i = 1, 2, \dots, m; j = 1, \dots, n$)

The weight for each attribute is supposed to be W_j in the third stage, where $j = 1, 2, \dots, n$. The weighted normalised (F) decision matrix is shown in (10) and the weights are calculated from AHP method.

$$F = W_j Q_{ij} \quad (10)$$

where

W_j = weights of individual input parameter (equal to 1)

The fourth stage allows for the determination of the positive (s^+) and negative (s^-) ideal solutions as given in (11) & (12).

$$S^+ = \left\{ \sum_i^{\min} (I_{ij} | j \in J) \left(\sum_i^{\min} (I_{ij} | j \in J | i = 1, 2, \dots, m) \right) \right\} \quad (11)$$

$$= F1+, F2+, F3+ \dots Fn+$$

$$S^- = \left\{ \sum_i^{\min} (I_{ij} | j \in J) \left(\sum_i^{\max} (I_{ij} | j \in J | i = 1, 2, \dots, m) \right) \right\} \quad (12)$$

$$= F1-, F2-, F3- \dots Fn-$$

The fifth stage is to get the Euclidean distance from the positive ideal solution (S_i^+) and the negative ideal solution (S_i^-), which are shown in (13) & (14).

$$S_i^+ = \sqrt{\sum_{j=1}^n (s_{ij} - s_j^+)^2}, i = 1, 2, 3, \dots, m \quad (13)$$

$$S_i^- = \sqrt{\sum_{j=1}^n (s_{ij} - s_j^-)^2}, i = 1, 2, 3, \dots, m \quad (14)$$

The final stage in TOPSIS is to get Nearness factor (H_i) as per (15).

$$H_i = \frac{S^-}{S^+ + S^-} \quad i = 1, 2, 3, \dots, m \quad (15)$$

The decision matrix and the weighted normalized matrix of the experiments used in this study are given in Table 8. The best and worst solutions for the output variables, viz., MRR, TWR, and SR are given in Table 9. and Table 10 shows the best and the worst solutions of the TOPSIS along with rank. Furthermore, ANN with a single hidden layer is employed to validate the actual Nearness factor, and the observations are shown in Table 11.

Table 8. Weighted normalized(F) values of MRR, TWR, and SR

S.No	Decision Matrix			Weighted Normalized (F)		
	MRR	TWR	SR	MRR	TWR	SR
1	1.1	0.06	6.44	0.136	0.025	0.068
2	0.45	0.12	10.82	0.056	0.050	0.114
3	1.18	0.08	9.37	0.146	0.033	0.099
4	1.89	0.27	7.19	0.233	0.112	0.076
5	1.55	0.27	9.50	0.191	0.112	0.100
6	0.61	0.09	8.77	0.075	0.037	0.093
7	2.53	0.3	7.07	0.312	0.125	0.075
8	0.38	0.07	8.76	0.047	0.029	0.092
9	0.73	0.05	11.84	0.090	0.021	0.125

Table 9. Best and worst solutions of MRR, TWR, and SR

S.No	Best Solution			Worst solution		
	MRR	TWR	SR	MRR	TWR	SR
1	0.031	0.000	0.000	0.008	0.000	0.000
2	0.066	0.001	0.002	0.000	0.001	0.002
3	0.028	0.000	0.001	0.010	0.000	0.001
4	0.006	0.008	0.000	0.035	0.008	0.000
5	0.015	0.008	0.001	0.021	0.008	0.001
6	0.056	0.000	0.001	0.001	0.000	0.001
7	0.000	0.011	0.000	0.070	0.011	0.000
8	0.070	0.000	0.001	0.000	0.000	0.001
9	0.049	0.000	0.003	0.002	0.000	0.003

Table 10. Estimating Nearness factor and ranking order

S.No	Euclidean distance from the best solution	Euclidean distance from worst solution	Nearness Factor (H_i)	Rank
1	0.176	0.089	0.335	5
2	0.262	0.055	0.174	7
3	0.170	0.104	0.380	4
4	0.121	0.208	0.632	2
5	0.155	0.174	0.529	3
6	0.239	0.041	0.147	8
7	0.104	0.285	0.733	1
8	0.266	0.026	0.089	9
9	0.229	0.072	0.238	6

Table 11. Actual & ANN Predicted Nearness Value

S.No	Nearness Factor-Actual	One Layer	
		Nearness Factor-ANN predicted	Error
1	0.619	0.6192999146	8.54E-08
2	0.590	0.3268401479	0.26315985
3	0.655	0.655100081	-8.10E-08
4	0.695	0.6785841758	0.01681582
5	0.174	0.1741000002	-1.59E-10
6	0.600	0.7002473776	-0.0998473
7	0.819	0.8193999837	1.63E-08
8	0.697	0.6978001627	-1.63E-07
9	0.403	0.4738931685	-0.07079316

3. RESULTS AND DISCUSSION

This section discusses the exploration of PMEDM of Inconel utilizing the Taguchi-based grey relational analysis (T-GRA) as well as the TOPSIS technique, the analysis of variance (ANOVA), and the main effects plot.

3.1 Multi-attribute decision-making using T-GRA and TOPSIS

The L_9 OA-based T-GRA and TOPSIS approaches have been used in the present experiment to identify the ideal process parameters for the given input parameters, viz., peak Current, Pulse on time, and Pulse off time. A higher response value for the T-GRA and TOPSIS can determine the optimal parametric combination. Higher GRG values will give the optimal factors to run the machining. Table 5 shows the highest GRG in experiment #7 for the given set of performance attributes, followed by runs #4 and #1. The design of experiment L_9 makes it simple to distinguish between the effects of various characteristics at different levels. The investigation shows that experimental #7 contains the three levels of process parameters used for machining in EDM to get a satisfied output response with both T-GRA & TOPSIS techniques. Therefore, the actual experiments, GRG (0.912), and Nearness factor (0.819) results are similar in output responses.

Table 12. Response of each factor of GRA and TOPSIS

S.No	Decision Matrix		Weighted Normalized (F)	
	GRG	Rank	Nearness Factor	Rank
1	0.529	3	0.619	5
2	0.286	8	0.59	7
3	0.332	5	0.655	4
4	0.654	2	0.695	3
5	0.507	4	0.174	9
6	0.328	6	0.600	6
7	0.912	1	0.819	1
8	0.315	7	0.697	2
9	0.260	9	0.403	8

Due to the current increase, the machining is improved with the ionization effect between the tool and the workpiece. Thus, the ionization effect increases with the increase of pulse-on time where temperature increases on the tool, which results in higher melting of

the workpiece, and the molten area is evaporated by heating during the pulse-off time, leading to higher MRR [42]. Moreover, the optimal value of SR is obtained, possibly due to the pressurized delivery of the powder dielectric. This flushes the debris away from the spark gap at the given pulse-off time [45]. Table 10 shows the best and the worst solutions of the TOPSIS along with rank, and the obtained ranks from the T-GRA and TOPSIS are shown in Table 12. It is observed from the T-GRG that experimental run #7 is the best for the experimental set-up. Also, the same experimental run #7 is the best ideal solution based on TOPSIS.

3.2 Main Effects Plot for GRG and Nearness Factor

Since the optimal process parameters are obtained based on MADM, the main effects plots for the GRG and nearness factor are given in Figures 5 and 6.

From Figure 5, the values of GRG increase with the increase in current and the pulse-on time, whereas pulse-off time drops down when it is increased. From the main effects plot of GRG, the optimal process parameters are 30 amps current, 20 μ Sec Pulse off time, and 9 μ Sec Pulse on time ($A_2-B_1-C_3$). The parameters improve at these levels since the plasma energy and the spark discharge are maximized at a high current and pulse on time. The work material is more likely to melt and evaporate under these conditions by flushing in the gap.

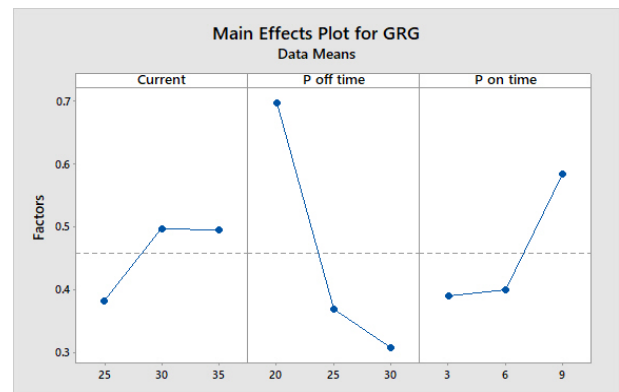


Figure 5. Main effects plot for GRG

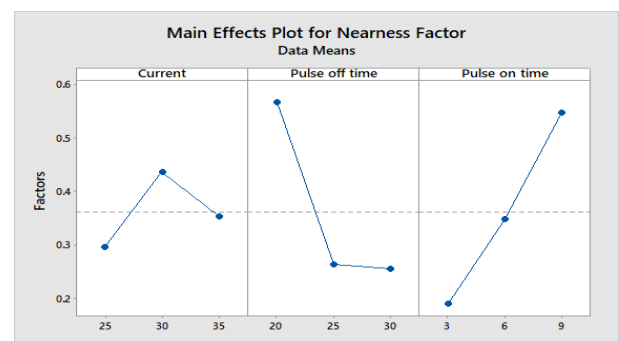


Figure 6. Main effects of the Nearness Factor

In the main effects plot for the nearness factor (Figure 6), a similar pattern occurs for the change in current, pulse-off time, and pulse-on time. The validation of the experimental procedure further strengthens these and further rationalizes the use of statistical methods. For TOPSIS, the ideal process parameters are found to be 30 amps current, 20 μ Sec Pulse off time, and 9 μ Sec Pulse on time ($A_2-B_1-C_3$). It is observed

from the optimal condition that the increase of current results in a higher plasma column, which leads to an increase in the spark energy during the machining of pulse off time[46].

From the ANOVA (Tables 13 and 14), it is understood that pulse-on time and pulse-off time are the contributing parameters to GRG as well as to the Nearness factor. Since the current, Pulse-on Time, and Pulse-off Time are used as three parameters, the factor which has the most contributing effect on these experiments and from Table 7, it is observed that the process parameter "Pulse-on time" has a higher importance than "Pulse-off time" and "current" when evaluating multiple-response processes. The regression equations referring to the GRG and Nearness factor are given as (16) & (17) respectively.

Table 13. ANOVA of GRG

S.No	Source	DF	Adj SS	Adj MS	F-value	P-value
1	Current	2	0.02584	0.01292	2.25	0.308
2	T _{off} time	2	0.26557	0.132785	23.08	0.042
3	T _{on} time	2	0.07107	0.035535	6.18	0.139
4	Error	2	0.01151	0.005753		
5	Total	8	0.37399			

Table 14. ANOVA of Nearness factor

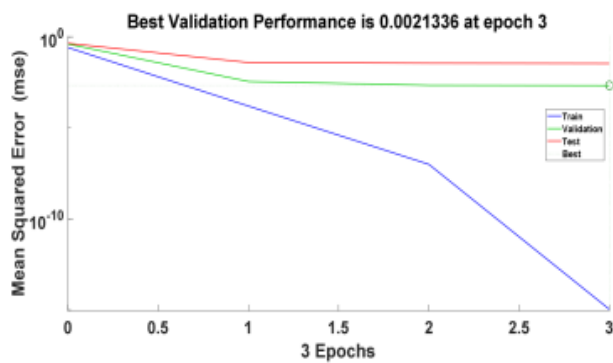
S.No	Source	DF	Adj SS	Adj MS	F-value	P-value
1	Current	2	0.02959	0.014795	59	0.017
2	T _{off} time	2	0.18882	0.094412	376.48	0.003
3	T _{on} time	2	0.19204	0.096021	382.89	0.003
4	Error	2	0.00050	0.000251		
5	Total	8	0.41095			

$$GRG = 0.904 + 0.01133 \text{ Current} + 0.03917 \text{ Pulse off time} + 0.0322 \text{ Pulse on Time} \quad (16)$$

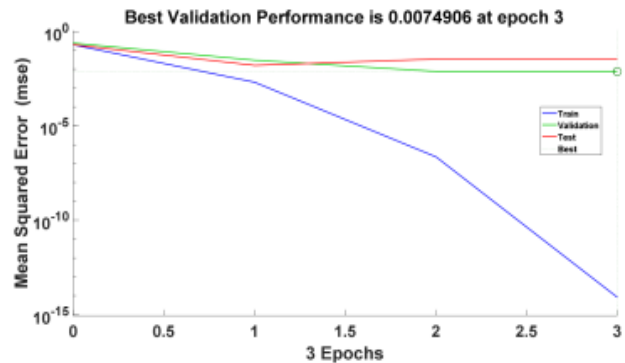
$$Hi = 0.613 + 0.00570 \text{ Current} - 0.03117 \text{ Pulse off time} + 0.0595 \text{ Pulse on Time} \quad (17)$$

3.3 Validation of GRG and Nearness factor by ANN

Since the results obtained from the MADM, main effects plots, and the ANOVA are satisfactory; it is decided to deploy ANN further to analyze the rank obtained in the previous sections. After entering all the 9 necessary data as input to the ANN model developed in MATLAB, the GRG, and the nearness factors are predicted with 5 input data for the training, followed by 2 for validation and the remaining 2 data for testing.



(a) GRG



(b) TOPSIS

Figure 9 (a & b) Performance Validation graph of GRG and Nearness factor

Based on the network scheme and the hidden layer mentioned in Figure 4, the values of GRG and nearness factor are predicted in Tables 6 and 11. To find the optimal neural network design, the level of error convergence has been studied by adjusting the quantity of hidden layers and the number of neurons in the hidden layers. Tables 6 and 11 show that the one-hidden-layer ANN network used in this study predicts the best GRG and nearness factor results based on the input parameters through a trial-and-error approach [47]. The designed network model predicts GRG values, which are compared with true-GRG values in Table 6.

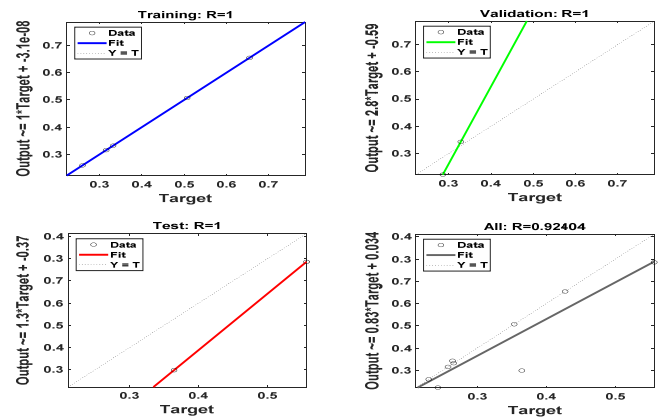


Figure 7. Network regression plot of GRA using ANN.

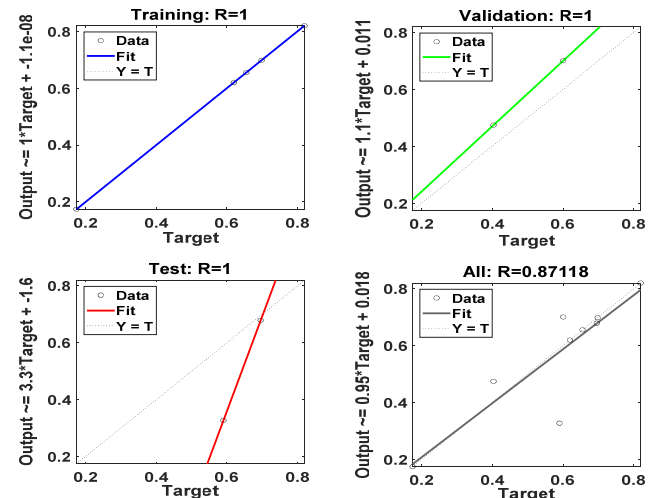


Figure 8. Network regression plot for Nearness factor using ANN

The designed neural network gives accurate predictions about parameters, and it shows that estimated GRG values and predicted GRG values are obtained with the least error. The ANN model has predicted the GRG with an R-value of 0.92404, as shown in Figure. 7. Similarly, the same ANN model has been utilized to predict the nearness factor and the R-value. The predicted value of the nearness factor is shown in Table 11. Furthermore, the ANN model predicts these nearness factors with an R-value of 0.87118, which is shown in Figure 8.

From the performance validation graph of these ANN models is shown in Figures. 9 (a) and 9 (b), the error in the ANN for predicting GRG and the nearness factor converges to zero at the end of the third iteration. The result elucidates that the created single-layered ANN has a truthful aptitude to predict the results even for ranks for the MADM methods. This developed ANN model will foresee the outcome of the experimental setup and can be practicably used to anticipate the expected outcome.

4. CONCLUSIONS

The paper has reported on applying the ANN technique in predicting results in multi-attribute decision-making viz., T-GRA and TOPSIS. To shun the use of one-step and two-step methods of mixing the powder in the dielectric, Eductor type PMEDM has been used in the machining of Inconel. The conclusions drawn from this study are:

- Optimization of multiple responses using T-GRA and TOPSIS for the given set of experiments identically points to experimental trial #7.
- The main effects plot for the T-GRA indicates the optimal factors as 30 amps current, 20 μ Sec Pulse off time, and 9 μ Sec Pulse on time. The same holds good for the TOPSIS as well.
- The outcome of the MADM results is further validated with the help of a single-layered ANN model. The developed ANN model has precisely predicted the GRG with an R-value of 0.92404; for the nearness factor, the R-value is 0.87118.
- As the proposed ANN model has been successful in predicting the MADM results, it has the potential to minimize the uncertainty among the data, resulting in better forecasting of characteristics performance in the multi-response optimization method.
- This ANN model limits the number of hidden layers and neurons. Moving further, the experiments can be enlarged with more factors with increased hidden layers of 2 or 3 and 100 neurons being used to increase the performance of ANN models.

LIST OF ACRONYMS AND ABBREVIATIONS

OA	Orthogonal Array
MRR	Material Removal Rate
TWR	Tool Wear rate
SR	Surface Roughness
PMEDM	Powder Mixed Electrical Discharge Machining
MADM	Multi-Attribute Decision Making

T-GRA	Taguchi- Grey Relational Analysis
TOPSIS	Technique for Order of Preference by Similarity to Ideal Solution
GRG	Grey Relational Grade
ANN	Artificial Neural Network
HL1	Hidden Layer 1

ACKNOWLEDGEMENTS

The authors thank B. S. Abdur Rahman Crescent Institute of Science and Technology for providing the facilities and infrastructure for conducting the experiments.

REFERENCES

- [1] Boothroyd, G. and Winston, A.K.: non-conventional machining processes, Fundam. mach. and mach. tools, 491,1989.
- [2] Ezeddini, S., Rajhi, W. and Boujelbene, O.: An Investigation to Achieve Good Surface Integrity in Wire Electrical Discharge Machining of Ti-6242 Super Alloy, J. of Mater. Eng. Perform., 2023.
- [3] Singh, M.R., Kumar, P.S. Singh, P.: Optimization of EDM process of titanium alloy using EPSDE technique, Multiscale and Multidiscip. Model. Exp. and Des., 4(2): p. 121-130, 2021.
- [4] Kalita, K., Chakraborty, S. Kumar, R.G.: Parametric optimization of non-traditional machining processes using multi-criteria decision making techniques: literature review and future directions, Multiscale and Multidiscip. Model. Exp. and Des., 6(1): p. 1-40 2023.
- [5] Hanif, M., Wasim, A. Shah, A.H.: Optimization of process parameters using graphene-based dielectric in electric discharge machining of AISI D2 steel, Int. J. Adv. Manuf. Technol. 103, 3735–3749, 2019.
- [6] Srinivasan, V.P, Rai, S.R. and Aruljothi, G.: Experimental investigation on electro discharge machining of aluminium alloy (Al 2024) using GRA, AIP Conf. proc., Vol. 2527, no.1, 2022.
- [7] Sen, G. and Mondal, S: Investigation of the effect of copper, brass and graphite electrode on electrical discharge machining of mild steel grade IS2062, AIP Conf. proc., Vol. 2273, 050054, 2020.
- [8] Jeswani M.L: Effect of the addition of graphite powder to kerosene used as the dielectric fluid in electrical discharge machining', wear, 70(2): p. 133-139, 1981.
- [9] Gugulothu, B., Krishna Mohana Rao, and Hanuantha Rao, D.: Experimental results on EDM of Ti-6Al-4V in drinking water with Graphite powder concentration, Mater. Today Proc., 46: pp. 234-242, 2020.
- [10] Jeavudeen, S., Sai Ram. J. and Pervaz Ahmed M.: Parameter optimization in the enhancement of MRR of titanium alloy using newer mixing method in PMEDM process, J. Eng. Appl. Sci. 70, 59, 2023.
- [11] Dhilip, J.D.J., Ganesan, K.P. Sivalingam, V.: Machinability Studies and Optimization of Process

- Parameters in Wire Electrical Discharge Machining of Aluminum Hybrid Composites by the VIKOR Method', *J. of Mater. Eng. and perform.*, 50, 2023.
- [12] Ahmad, S., Lajis, M.A.: Electrical discharge machining (EDM) of Inconel 718 by using copper electrode at higher peak current and pulse duration, *IOP Conf. Ser. Mater. Sci. Eng.* 50, 012062, 2013.
- [13] Singh, A., Ghadai, R.K. and Kalita, K.: EDM process parameter optimization for efficient machining of INCONEL-718', *Facta Universitatis, Ser. Mech. Eng.*, Volume 18 (3), pp. 473-490, 2020.
- [14] Payal, H., Endale, F., Bhattacharya, A.: Optimization of machining parameters in EDM of Inconel 625 using Taguchi approach, *Mater. Today Proc.*, Vol. 80 (2), pp. 1422-1428, 2023.
- [15] Bharti, P., Maheshwari, Sharma, C.S.: Experimental investigation of Inconel 718 during die-sinking electric discharge machining, *Int. J. Eng. Sci. Tech*, Vol. 2, pp. 6464-6473, 2010.
- [16] Hussain, A., Sharma, A.K., Singh, J.P.: Maximizing MRR of Inconel 625 machining through process parameter optimization of EDM', *Mater. Today Proc.*, Vol. 79 (2): pp. 303-307, 2023.
- [17] Dar, A. and Anuradha, N.: Use of orthogonal arrays and design of experiment via Taguchi L9 method in probability of default, *Accounting*, Vol. 4(3): pp. 113-122, 2017.
- [18] Balakrishnan, D., Anantha Raman, L., Senthil-kumar, N., and Shivasankar, J.: Investigation and Optimization of Machining Parameters Influence on Surface Roughness in Turning AISI 4340 Steel, *FME Trans.*, Vol. 48 (2), pp. 383-390, 2020.
- [19] Srinivasan, V.P, Duraithilagar, S. Dhanasekhar, S.: Optimization of electrical discharge machining process parameters of titanium alloy using Taguchi methodology, *AIP Conf. proc.*, Vol. 2527, 2022.
- [20] Singh, K., Singh, A.K., Chattopadhyay, K.D.: Optimization of tool wear rate during EDM of HSLA steel, *Mater. Today Proc.*, Vol. 69(2), pp. 361-364, 2022
- [21] Ramamurthy, A., Sivaramakrishnan, R., Muthuramalingam, T.: Performance Analysis of Wire Electrodes on Machining Ti-6Al-4V Alloy using Electrical Discharge Machining Process, *Mach. Sci. and Technol.*, Vol. 19(4): p. 577-592, 2015.
- [22] Hadiand, M., & Ibrahim, A.: Effect of copper-graphite composite electrode on material removal rate and surface roughness in MONEL 400 during electrical discharge machining, *Metall. Mater. Eng.*, Vol. 28(2): p. 245-255, 2022.
- [23] Jeavudeen, S., Jailani, H.S., Murugan M.: Influence of thermo-electrical property of materials on powder mixed electrical discharge machining, *FME Trans.*, Vol. 47(3):518-23, 2019.
- [24] Kumar Mohanty, U., Rana, J., Sharma, A.: multi-objective optimization of electro-discharge machining (EDM) parameter for sustainable machining, *Mater. Today Proc.*, Vol. 4(8), pp. 9147-9157, 2017.
- [25] Dewangan, S.K., Kumar, P., Jha, S.K.: Optimization of Quality and Productivity of Wire EDM by Using L9 Orthogonal Array, *Adv. Ind. Prod. Eng.*, 2019.
- [26] Mandal, P., Mondal, S.C.: Investigation on the Performance of Copper-Coated 6061 Aluminium Alloy Electrode in Electric Discharge Machining, *Res. Des. for a Connected World*, 2019.
- [27] Mukherjee, S., Rai, D., Giridharan, A.: EDM of titanium foam: electrode wear rate, oversize, and MRR, *Mater. Manuf. Processes*, Vol. 37(7): pp. 825-837, 2022.
- [28] Balasubramanian, P., Thiyagarajan, S.: Optimization of Machining Parameters in EDM Process Using Cast and Sintered Copper Electrodes, *Procedia Mater. Sci.*, Vol. 6, pp. 1292-1302, 2014.
- [29] Yuangang, W., Naiyang, H., Xiaopeng, L.: Segmented manufacturing of micro-electrode based on EDM and its performance evaluation, *Procedia CIRP*, 113: p. 81-86, 2022.
- [30] Singh, R.K., Swati, G., Singh, D.K.: Exploration of GRA Based Multiobjective Optimization of Magnetic Abrasive Finishing Process using Simulated Annealing, *FME Trans.*, Vol. 48, pp. 195-203, 2020.
- [31] Kumar, D., Mondal, S.: (2020), 'Process parameters optimization of AISI M2 steel in EDM using Taguchi based TOPSIS and GRA, *Mater. Today Proc.*, Vol. 26(2), pp. 2477-2484, 2020.
- [32] Srinivasan, V.P, Palani, P.K., Balamurugan, S.: Experimental investigation on EDM of Si3N4-TiN using grey relational analysis coupled with teaching-learning-based optimization algorithm, *Ceram. Int.*, Vol. 47(13), pp. 19153-19168, 2021.
- [33] Rajamanickam, S., Prasanna, J.: Multi Objective Optimization during Small Hole Electrical Discharge Machining (EDM) of Ti-6Al-4V using TOPSIS, *Mater. Today Proc.*, Vol. 18, pp. 3109-3115, 2019.
- [34] Bhaumik, M., Maity, K., Mohapatra, K.: Multi-objective optimization of edm process parameters using RSM-based GRA and TOPSIS method for grade 6 titanium alloy, *Surf. Rev. Lett.*, Vol. 28, p. 2150062, 2021.
- [35] Wang, K., Gelgele, H.L., Wang, Y.: A hybrid intelligent method for modelling the EDM process, *Int. J. Mach. Tools Manuf.*, Vol. 43(10), pp. 995-999, 2003.
- [36] Dimla, D.E., Lister, P.M., Leighton, N.J.: Neural network solutions to the tool condition monitoring problem in metal cutting—A critical review of methods, *Int. J. Mach. Tools Manuf.*, Vol. 37(9), pp. 1219-1241, 1997.
- [37] Tsai, K.M., Wang, P.J.: Predictions on surface finish in electrical discharge machining based upon neural network models, *Int. J. Mach. Tools Manuf.*, Vol. 41(10), p. 1385-1403, 2001.
- [38] Somachai, K., Sonthipermpon, K., Kielarova, S.W: Springback Optimization for CNC Tube Bending Machine Based on an Artificial Neural

- Networks (ANNs), FME Trans., Vol. 51, pp.404-413, 2023.
- [39] Sabaei, D., Erkoyuncu, J. and Roy, R.: A Review of Multi-criteria Decision-Making Methods for Enhanced Maintenance Delivery, Procedia CIRP, Vol. 37, p. 30-35, 2015.
- [40] Madic, M. J., Radovanovic, M. R.: Optimal Selection of ANN Training and Architectural Parameters Using Taguchi Method: A Case Study, FME Trans., Vol. 39, pp.79-86, 2011.
- [41] Karatas, C., Sozen, A., Dulek, E.: Modelling of residual stresses in the shot peened material C-1020 by artificial neural network, Expert Syst. Appl., Vol. 36(2), p. 3514-3521, 2009.
- [42] Muthuramalingam, T., Mohan, B.: Application of Taguchi-grey multi responses optimization on process parameters in electro erosion, Meas., Vol. 58, p. 495-502, 2014.
- [43] Sapuan, S.M., Mujtaba, I.: *Composite materials technology*, Neural network applications, 1-355, 2005.
- [44] Bhuyan, R.K., Routara, B.C., Kumar Parida, A.: An approach for optimization the process parameter by using TOPSIS Method of Al-24%SiC metal matrix composite during EDM, Mater. Today Proc., Vol. 2(4), p. 3116-3124, 2015.
- [45] Huu, P.N.: Multi-objective optimization in titanium powder mixed electrical discharge machining process parameters for die steels, Alexandria Eng. J., Vol. 59(6), p. 4063-4079, 2020.
- [46] Che Haron, C.H. et al.: Copper and graphite electrodes performance in electrical-discharge machining of XW42 tool steel, J. Mater. Process. Technol., Vol. 201(1), p. 570-573, 2008.
- [47] Uyyala, S., Kumar, A., Krishna, A.: Performance analysis of electrical discharge machining parameters on RENE 80 nickel super alloy using statistical tools, Int. J. Mach. Mach. Mater., Vol. 15, pp. 212-234, 2014.

**ОПТИМИЗАЦИЈА ПМЕДМ СА ВИШЕ
ОДГОВОРА НА ИНКОНЕЛ 718 КОРИСТЕЊИ
ХИБРИДНИ Т-ГРА, ТОПСИС И АНН МОДЕЛ**

Ц.С. Рам, Ц. Шиек, Ш.Х. Сјед

Инконел 718 је једна од суперлегура на бази никла, која се сматра једним од најтежих материјала за машинску обраду због своје особине да задржи тврдоћу на вишим температурама. Ова студија је испитала перформансе ПМЕДМ обраде засноване на Едцитор-у на Инконел 718. Тагучи Л9 ОА је коришћен са струјом, временом искључења импулса и временом укључивања импулса као параметри процеса са притиском на страни испоруке од 6 бара за мешани диелектрик глинице. Стопа уклањања материјала (МРР), стопа хабања алата (ТВР) и хрпаваост површине (СР) су узете као излазни одговори. Резултати су истражени МАДМ техникама, односно Taguchi-based Grey Analysis (Т-ГРА) & ТОПСИС анализа. Штавише, рангови добијени од Т-ГРА & ТОПСИС су потврђени развојем једнослојног АНН модела. Рангови предвиђени АНН моделом су исти за Т-ГРА и ТОПСИС, а Р-вредности су 0,924 и 0,871, респективно. АНОВА је такође коришћена за анализу ефеката параметара на излазне одговоре.